

REPORT DOCUMENTATION PAGE			Form Approved OMB NO. 0704-0188		
<p>The public reporting burden for this collection of information is estimated to average 1 hour per response, including the time for reviewing instructions, searching existing data sources, gathering and maintaining the data needed, and completing and reviewing the collection of information. Send comments regarding this burden estimate or any other aspect of this collection of information, including suggestions for reducing this burden, to Washington Headquarters Services, Directorate for Information Operations and Reports, 1215 Jefferson Davis Highway, Suite 1204, Arlington VA, 22202-4302. Respondents should be aware that notwithstanding any other provision of law, no person shall be subject to any penalty for failing to comply with a collection of information if it does not display a currently valid OMB control number.</p> <p>PLEASE DO NOT RETURN YOUR FORM TO THE ABOVE ADDRESS.</p>					
1. REPORT DATE (DD-MM-YYYY) 12-06-2014		2. REPORT TYPE Final Report		3. DATES COVERED (From - To) 1-Sep-2011 - 28-Feb-2014	
4. TITLE AND SUBTITLE Pressure-induced Formation of Energetic and Structural Extended Solids with Quench-recovery to Ambient Conditions				5a. CONTRACT NUMBER W911NF-11-1-0300	
				5b. GRANT NUMBER	
				5c. PROGRAM ELEMENT NUMBER 1D10BO	
				5d. PROJECT NUMBER	
6. AUTHORS T.A. Strobel, M. Somayazulu, R.J. Hemley, O.O. Kurakevych				5e. TASK NUMBER	
				5f. WORK UNIT NUMBER	
7. PERFORMING ORGANIZATION NAMES AND ADDRESSES Carnegie Institution of Washington 1530 P Street NW  Washington, DC 20005 -1910				8. PERFORMING ORGANIZATION REPORT NUMBER	
9. SPONSORING/MONITORING AGENCY NAME(S) AND ADDRESS (ES) U.S. Army Research Office P.O. Box 12211 Research Triangle Park, NC 27709-2211				10. SPONSOR/MONITOR'S ACRONYM(S) ARO	
				11. SPONSOR/MONITOR'S REPORT NUMBER(S) 60587-EG-DRP.8	
12. DISTRIBUTION AVAILABILITY STATEMENT Approved for Public Release; Distribution Unlimited					
13. SUPPLEMENTARY NOTES The views, opinions and/or findings contained in this report are those of the author(s) and should not be construed as an official Department of the Army position, policy or decision, unless so designated by other documentation.					
14. ABSTRACT Carbon clathrate materials, comprised of sp <sup>3</sup> carbon structures with light elements, as well as polymeric carbon monoxide, represent two classes of high-pressure materials with promising potential structural and energetic applications. A systematic exploration of PT <sub>x</sub> space was performed in carbon+ alkali and alkaline earth metals, under high-pressure/temperature conditions, as well as silicon-based systems, to establish the propensity to form sp <sup>3</sup> -based carbon/silicon networks with superlative properties. For the case of silicon, it was unambiguously determined that silicon clathrates are thermodynamically stable at high pressure conditions. This suggests that other high					
15. SUBJECT TERMS high pressure, synthesis, clathrate, poly-CO					
16. SECURITY CLASSIFICATION OF:			17. LIMITATION OF ABSTRACT UU	15. NUMBER OF PAGES	19a. NAME OF RESPONSIBLE PERSON Timothy Strobel
a. REPORT UU	b. ABSTRACT UU	c. THIS PAGE UU			19b. TELEPHONE NUMBER 202-478-8943

## Report Title

### Pressure-induced Formation of Energetic and Structural Extended Solids with Quench-recovery to Ambient Conditions

#### ABSTRACT

Carbon clathrate materials, comprised of sp<sup>3</sup> carbon structures with light elements, as well as polymeric carbon monoxide, represent two classes of high-pressure materials with promising potential structural and energetic applications. A systematic exploration of PT<sub>x</sub> space was performed in carbon+ alkali and alkaline earth metals, under high-pressure/temperature conditions, as well as silicon-based systems, to establish the propensity to form sp<sup>3</sup>-based carbon/silicon networks with superlative properties. For the case of silicon, it was unambiguously determined that silicon clathrates are thermodynamically stable at high-pressure conditions. This suggests that other high-pressure phases may be synthesized outside their thermodynamic stability regime and elucidates the first example of the chemical synthesis of a high-pressure phase at ambient-pressure conditions. We examined the sodium removal from a newly discovered NaSi<sub>6</sub> (Na<sub>4</sub>Si<sub>24</sub>) compound. Upon complete sodium removal, a new sp<sup>3</sup> silicon allotrope was produced that possesses a quasidirect band gap with the ideal value for photovoltaic applications. For the case of carbon, mixtures with Li, Mg, Na, and Ca were investigated. All systems showed known carbide formation under certain conditions, but several new and recoverable phases were identified including Mg<sub>2</sub>C, Mg<sub>2</sub>C<sub>3</sub>, Ca<sub>2</sub>C, Ca<sub>2</sub>C<sub>3</sub> and Ca<sub>3</sub>C<sub>2</sub>. Some of these, such as Mg<sub>2</sub>C, contain unusual anions like C<sub>4</sub><sup>-</sup> that are recoverable to ambient conditions and display sp<sup>3</sup> carbon hybridization. These may serve as useful precursors for carbon clathrate materials. The polymerization behavior of CO (poly-CO, p-CO) was examined over a range of conditions with different dopants. The presence of molecular nitrogen and acetylene did not significantly affect the polymerization pressure of CO or the molecular structure of the resulting polymer. The presence of amorphous carbon and SiO<sub>2</sub> appear to reduce the polymerization pressure by a fraction of one GPa. The presence of metallic lithium and sodium appear to reduce the polymerization pressure substantially. These additives may be considered as a route to producing larger quantities of p-CO.

**Enter List of papers submitted or published that acknowledge ARO support from the start of the project to the date of this printing. List the papers, including journal references, in the following categories:**

**(a) Papers published in peer-reviewed journals (N/A for none)**

Received

Paper

- |            |      |  |
|------------|------|--|
| 06/12/2014 | 6.00 | Oleksandr O. Kurakevych, Yann Le Godec, Timothy A. Strobel, Duck Young Kim, Wilson A. Crichton, J  r  my Guignard. High-Pressure and High-Temperature Stability of Antifluorite Mg, The Journal of Physical Chemistry C, (04 2014): 0. doi: 10.1021/jp5010314            |
| 08/29/2013 | 2.00 | Oleksandr O. Kurakevych, Timothy A. Strobel, Duck Young Kim, Takaki Muramatsu, Viktor V. Struzhkin. Na-Si Clathrates Are High-Pressure Phases: A Melt-Based Route to Control Stoichiometry and Properties, Crystal Growth & Design, (01 2013): 0. doi: 10.1021/cg3017084 |
| 08/29/2013 | 3.00 | George D. Cody, Oleksandr O. Kurakevych, Timothy A. Strobel, Duck Young Kim. Synthesis of Mg <sub>2</sub> C: A Magnesium Methanide, Angewandte Chemie International Edition, (08 2013): 0. doi: 10.1002/anie.201303463   |

**TOTAL: 3**

Number of Papers published in peer-reviewed journals:

---

(b) Papers published in non-peer-reviewed journals (N/A for none)

<u>Received</u>	<u>Paper</u>
-----------------	--------------

TOTAL:

Number of Papers published in non peer-reviewed journals:

---

(c) Presentations

- 1) High Pressure Gordon Research Conference, Biddeford, ME, June 24-29, 2012
- 2) Atomic and Intermolecular Interactions Gordon Research Conference, Easton, MA July 15-20, 2012
- 3) Strobel, T.A., Neighborhood Public Lecture, Carnegie Institution of Washington, Washington, DC (2012).
- 4) Strobel, T.A., Chemical Engineering Departmental Seminar, Colorado School of Mines, Golden, CO (2013).
- 5) Strobel, T.A., Chemistry Departmental Seminar, Naval Research Laboratory, Washington, DC (2013).
- 6)Kurakevych, O.O.; Le Godec, Y.; Strobel, T.A.; Turkevich, V.Z.; Solozhenoko, V.L., IUCrWorkshop: Advances in Static and Dynamic High-Pressure Crystallography, Hamburg, Germany (2013).

Number of Presentations: 6.00

---

Non Peer-Reviewed Conference Proceeding publications (other than abstracts):

<u>Received</u>	<u>Paper</u>
-----------------	--------------

TOTAL:

Number of Non Peer-Reviewed Conference Proceeding publications (other than abstracts):

---

Peer-Reviewed Conference Proceeding publications (other than abstracts):

<u>Received</u>	<u>Paper</u>
-----------------	--------------

TOTAL:

(d) Manuscripts

<u>Received</u>	<u>Paper</u>
06/12/2014	7.00 Timothy A. Strobel, <sup>†,*</sup> , Oleksandr O. Kurakevych, <sup>†,‡</sup> , Duck Young Kim, <sup>†</sup> , Yann Le Godec, <sup>‡</sup> , Wilson Crichton, <sup>§</sup> , Jérémy Guignard, <sup>§</sup> , Nicolas Guignot, <sup>?</sup> , George D. Cody <sup>†</sup> , Artem R. Oganov. Synthesis of ??Mg2C3: A Monoclinic High-Pressure Polymorph of2 Magnesium Sesquicarbide, Inorganic Chemistry (02 2014)
08/29/2013	4.00 DuckYoung Kim, Stevce Stefanoski, Oleksandr O. Kurakevych, Timothy A. Strobel. A new allotrope of silicon with a quasidirect band gap, To be submitted for publication (08 2013)
08/30/2012	1.00 Oleksandr O. Kurakevych, Timothy A. Strobel, Duck Young Kim, Takaki Muramatsu, Viktor V. Struzhkin. Na-Si Clathrates are high-pressure phases: A melt-based route to control stoichiometry and properties, SUBMITTED (07 2012)
<b>TOTAL:</b>	<b>3</b>

Number of Manuscripts:

---

Books

<u>Received</u>	<u>Book</u>
-----------------	-------------

**TOTAL:**

<u>Received</u>	<u>Book Chapter</u>
-----------------	---------------------

**TOTAL:**

## Patents Submitted

U.S. Provisional App. No. 61/843,581, filed July 8, 2013, and U.S. Provisional App. No. 61/874,582, filed September 6, 2013.

---

## Patents Awarded

---

### Awards

- (1) Invited lecture at Atomic and Intermolecular Interactions Gordon Research Conference, Easton, MA July 15-20, 2012.
- 
- (2) Mg<sub>2</sub>C publication (Angewandte Chemie) featured on inside back cover
- 

### Graduate Students

<u>NAME</u>	<u>PERCENT SUPPORTED</u>
<b>FTE Equivalent:</b>	
<b>Total Number:</b>	

---

### Names of Post Doctorates

<u>NAME</u>	<u>PERCENT SUPPORTED</u>
Oleksandr Kurakevych	1.00
<b>FTE Equivalent:</b>	<b>1.00</b>
<b>Total Number:</b>	<b>1</b>

---

### Names of Faculty Supported

<u>NAME</u>	<u>PERCENT SUPPORTED</u>
<b>FTE Equivalent:</b>	
<b>Total Number:</b>	

---

### Names of Under Graduate students supported

<u>NAME</u>	<u>PERCENT SUPPORTED</u>
<b>FTE Equivalent:</b>	
<b>Total Number:</b>	

### Student Metrics

This section only applies to graduating undergraduates supported by this agreement in this reporting period

The number of undergraduates funded by this agreement who graduated during this period: ..... 0.00

The number of undergraduates funded by this agreement who graduated during this period with a degree in science, mathematics, engineering, or technology fields:..... 0.00

The number of undergraduates funded by your agreement who graduated during this period and will continue to pursue a graduate or Ph.D. degree in science, mathematics, engineering, or technology fields:..... 0.00

Number of graduating undergraduates who achieved a 3.5 GPA to 4.0 (4.0 max scale):..... 0.00

Number of graduating undergraduates funded by a DoD funded Center of Excellence grant for Education, Research and Engineering:..... 0.00

The number of undergraduates funded by your agreement who graduated during this period and intend to work for the Department of Defense ..... 0.00

The number of undergraduates funded by your agreement who graduated during this period and will receive scholarships or fellowships for further studies in science, mathematics, engineering or technology fields: ..... 0.00

### Names of Personnel receiving masters degrees

NAME

**Total Number:**

### Names of personnel receiving PHDs

NAME

**Total Number:**

### Names of other research staff

NAME

PERCENT SUPPORTED

**FTE Equivalent:**

**Total Number:**

### Sub Contractors (DD882)

### Inventions (DD882)

## Scientific Progress

We have investigated the high-pressure / high-temperature (HP / HT) synthesis of novel structural and energetic solids, based on carbon and oxygen-carbon frameworks, which are expected to exhibit exceptional materials properties, show ambient quench recoverability and have potential for larger-volume scaling. We have examined a broad range of PTx conditions in the carbon (silicon) + alkali or alkaline earth metal systems to determine the extent of HP compound formation, ambient recoverability and new materials properties. We have investigated the polymerization of carbon monoxide (p-CO) under HP conditions in the presence of dopants and catalytic additives to determine effect on polymerization onset pressure and chemical stability.

Summary of the most important results are enumerated below as concise conclusions, supporting discussion with tables & figures are provided in the attached document.

- 1) Sodium-silicon clathrates are HP phases. This indicates that HP phases may be synthesized through chemical precursors at ambient conditions.
- 2) A new structure, NaSi<sub>6</sub>, was discovered at HP. This phase is recoverable to ambient conditions and shows unusual, potentially quasi-one-dimensional, electrical resistivity.
- 3) By treating a NaSi<sub>6</sub> precursor compound (Na<sub>4</sub>Si<sub>24</sub> unit cell) we were able to produce a new pure allotrope of silicon (Si<sub>24</sub>) that has a quasidirect band gap.
- 4) Carbon + light metal systems show rich behavior under HP/HT conditions. Several previously unreported structures and compounds were discovered.
- 5) A new carbide, Mg<sub>2</sub>C, was discovered at HP/HT conditions. This phase is fully recoverable to ambient conditions. It has a bulk modulus of 87 GPa and is electrically insulating. This compound could potentially act as a solid-based fuel source as it is readily hydrolyzed to form CH<sub>4</sub> gas.
- 6) The thermodynamic properties of Mg<sub>2</sub>C were established and the conditions of high-pressure, high-temperature stability have been determined.
- 7) A new polymorph of Mg<sub>2</sub>C<sub>3</sub> carbide was discovered and the crystal structure was solved using a combination of experimental and theoretical methods.
- 8) New structures in the Ca+C system were identified. Some of these may contain unique polymeric carbon units.
- 9) Methods were developed to prepare samples of p-CO. This can be done routinely for samples with dimensions of 1000 micron diameter x 150 micron thickness.
- 10) The polymerization pressure of CO in the presence of N<sub>2</sub> and C<sub>2</sub>H<sub>4</sub> is not reduced from the pure CO sample conditions. These dopants tend to phase separate with no significant alteration of the chemical structure; however, subtle vdW-type interaction was observed.
- 11) Neither seed crystals of p-CO nor nano-sized Pd powder reduce the pressure required for CO polymerization at ambient temperature.
- 12) Amorphous carbon appears to reduce the polymerization onset pressure of CO by ~0.5 GPa when compared with the pure system. It is unclear whether this is a catalytic (nucleation) or thermodynamic (chemical stabilization) effect.
- 13) The polymerization pressure of CO was investigated in the presence of several different metal and non-metal catalysts. Metallic lithium and sodium, as well as non-metallic amorphous carbon and SiO<sub>2</sub>, appear to reduce the pressure needed for CO polymerization.

## Technology Transfer

## Final Report

### Attachment: Discussion and figures

Proposal Number: 60587EGDRP

Agreement Number: W911NF1110300

Proposal Title: Pressure-induced Formation of Energetic and Structural Extended Solids with Quench-recovery to Ambient Conditions

Report Period Begin Date: 09/01/2012

Report Period End Date: 02/28/2014

T.A. Strobel, M. Somayazulu, R.J. Hemley, O.O. Kurakevych

### Abstract

Carbon clathrate materials, comprised of  $sp^3$  carbon structures with light elements, as well as polymeric carbon monoxide, represent two classes of high-pressure materials with promising potential structural and energetic applications. A systematic exploration of PTx space was performed in carbon+ alkali and alkaline earth metals, under high-pressure/temperature conditions, as well as silicon-based systems, to establish the propensity to for  $sp^3$ -based carbon/silicon networks with superlative properties. For the case of silicon, it was unambiguously determined that silicon clathrates are thermodynamically stable at high-pressure conditions. This suggests that other high-pressure phases may be synthesized outside their thermodynamic stability regime and elucidates the first example of the chemical synthesis of a high-pressure phase at ambient-pressure conditions. We examined the sodium removal from a newly discovered  $NaSi_6$  ( $Na_4Si_{24}$ ) compound. Upon complete sodium removal, a new  $sp^3$  silicon allotrope was produced that possesses a quasidirect band gap with the ideal value for photovoltaic applications. For the case of carbon, mixtures with Li, Mg, Na, and Ca were investigated. All systems showed known carbide formation under certain conditions, but several new and recoverable phases were identified including  $Mg_2C$ ,  $Mg_2C_3$ ,  $Ca_2C$ ,  $Ca_2C_3$  and  $Ca_3C_2$ . Some of these, such as  $Mg_2C$ , contain unusual anions like  $C^{4-}$  that are recoverable to ambient conditions and display  $sp^3$  carbon hybridization. These may serve as useful precursors for carbon clathrate materials. The polymerization behavior of CO (poly-CO, p-CO) was examined over a range of conditions with different dopants. The presence of molecular nitrogen and acetylene did not significantly affect the polymerization pressure of CO or the molecular structure of the resulting polymer. The presence of amorphous carbon and  $SiO_2$  appear to reduce the polymerization pressure by a fraction of one GPa. The presence of metallic lithium and sodium appear to reduce the polymerization pressure substantially. These additives may be considered as a route to producing larger quantities of p-CO.

### Scientific progress and accomplishments

#### 1) Sodium-silicon clathrates are HP phases. This indicates that HP phases may be synthesized through chemical precursors at ambient conditions.

For the first time we have demonstrated unambiguously that Na+Si clathrates are thermodynamically stable high-pressure phases. Sodium clathrates were prepared from elemental Na/Si mixtures (20 at% of Na, i.e., ~5% excess as compared with stoichiometric sI and sII clathrates) using the multi-anvil press technique at pressures between 1-8 GPa and temperatures between 700-1275 K. Figure 1 shows the x-ray diffraction pattern obtained from a sample that was recovered from 6 GPa and 1100 K. The x-ray diffraction pattern indicates that



sI clathrate may be synthesized directly from the elements under HP/HT conditions. In addition we have performed DFT calculations that confirm the high-pressure thermodynamic stability.

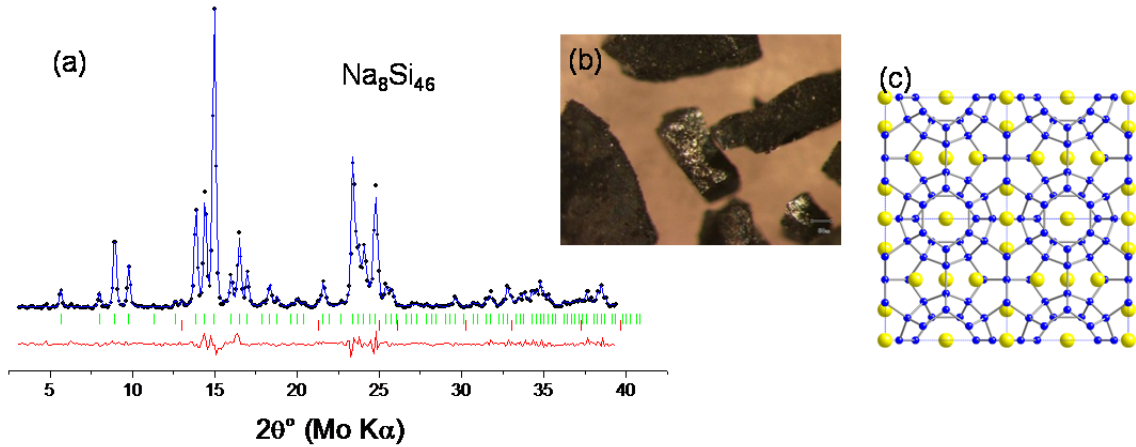


Figure 1. (a) X-ray diffraction pattern of sI clathrate synthesized at 6 GPa and 1100K. (b) Images of metallic sI ( $\text{Na}_8\text{Si}_{46}$ ), scale bar is 50 microns. (c) atomic structure of sI clathrate.

These results open new perspectives for high-pressure synthesis and properties control of new advanced materials. The high-pressure thermodynamic stability of Na-Si clathrate phases allows for a melt-based synthesis approach, which could be very useful for compositional control in mixed phases (e.g., Na+Ba etc.), high-quality single crystals, and for precise tuning of the occupancy ratios. All phases formed in this pressure domain allow for larger-volume scaling of materials (from 40  $\text{cm}^3$  for cubic sI at  $\sim 3$  GPa to 1  $\text{cm}^3$  at  $\sim 8$  GPa). Our results reveal the existence of multiple chemical mechanisms that allow for synthesis of high-pressure phases “without pressure”. Because the thermodynamic stability fields of Na-Si clathrate phases only exist under high-pressure conditions, previous reports of these structures may be viewed as non-equilibrium, precursor-based syntheses of high-pressure phases at low-pressure conditions. The understanding of such intrinsic interrelationships between thermodynamics and kinetics is thus the next step to explore that could open potential for other precursor-based synthesis of other high-pressure phases, especially carbon-based materials. Na-Si clathrate formation may be viewed as the first chemical example of a high-pressure phase at ambient conditions.

## 2) A new structure, $\text{NaSi}_6$ , was discovered at HP. This phase is recoverable to ambient conditions and shows unusual, potentially quasi-one-dimensional, electrical resistivity.

During the synthesis of Na+Si clathrate phases, the formation of a novel Na-Si compound,  $\text{NaSi}_6$  was observed when pressure was increased to 8 GPa. It has the  $\text{Eu}_4\text{Ga}_8\text{Ge}_{16}$  structural type (Fig. 2), never reported thus far for an alkali metal. The structure is composed of  $\text{sp}^3$ -bonded Si atoms, which form tunnels, intercalating Na atoms along the  $a$ -axis. As compared to  $\text{BaSi}_6$ ,  $\text{SrSi}_6$ , and  $\text{CaSi}_6$ , the corresponding sodium compound forms at substantially lower pressure: 8 GPa as compared to 11.5 GPa and 10 GPa for  $\text{BaSi}_6$  and  $\text{CaSi}_6$ , respectively. The pressure for  $\text{NaSi}_6$  formation allows consideration of this phase for a large-volume production, e.g., in the toroid-type high-pressure systems, contrary to similar compounds of alkali-earth metals.

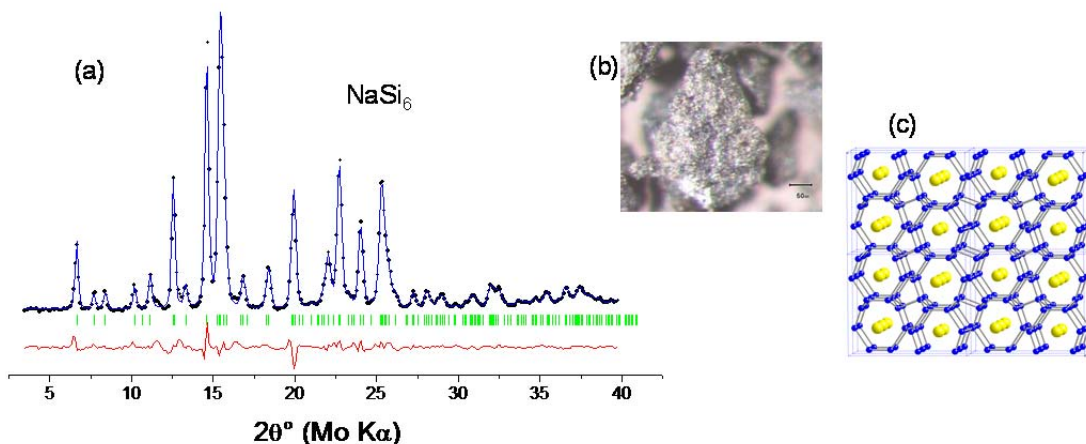


Figure 2. (a) X-ray diffraction pattern of NaSi<sub>6</sub> at 8 GPa and 1100K. (b) Images of metallic NaSi<sub>6</sub>, scale bar is 50 microns. (c) Atomic structure of NaSi<sub>6</sub>.

The electrical resistivity of NaSi<sub>6</sub> as a function of temperature was measured by the standard four-electrode technique, using a Physical Property Measurement System (PPMS: Quantum Design, Inc.). Overall, NaSi<sub>6</sub> exhibits metallic behavior, with the electrical resistivity increasing approximately as a parabolic curve with temperature above 75 K (Fig. 3). Below 75 K, the electrical resistivity begins to increase with further temperature decrease, a feature never observed so far for related compounds within this structural family. The observed minimum at about 75 K might be caused by the complexity of the electronic band structure, particularly the one-dimensional nature of the Na channels, or an unknown magnetic scattering process.

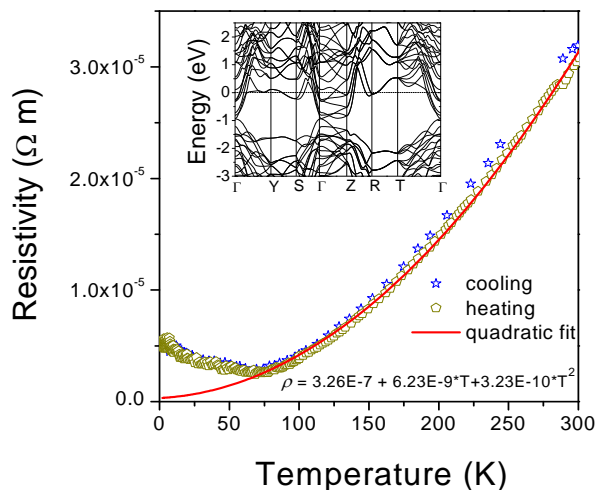


Figure 3. Electrical resistivity of NaSi<sub>6</sub> as a function of temperature. Inset shows the calculated band structure at 1 MPa.

### 3) By treating a NaSi<sub>6</sub> precursor compound (Na<sub>4</sub>Si<sub>24</sub> unit cell) we were able to produce a new pure allotrope of silicon (Si<sub>24</sub>) that has a quasidirect band gap.

Previously, we demonstrated unambiguously that Na+Si clathrates are thermodynamically stable high-pressure phases, and also reported the discovery of a new NaSi<sub>6</sub> (Na<sub>4</sub>Si<sub>24</sub> unit cell) compound. This compound consists of a channel-like sp<sup>3</sup> silicon host structure with chains of

sodium atoms as a guest structure. These open channels that host sodium atoms suggest a possible pathway for sodium removal via diffusion along the channels as schematically shown in Figure 4.

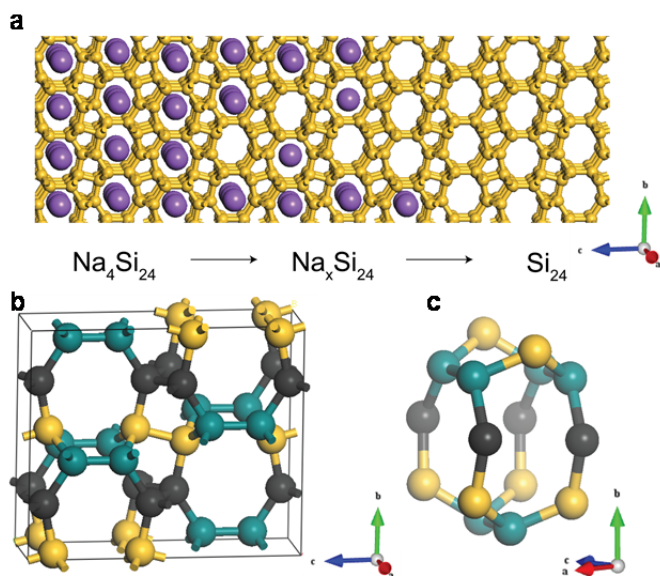


Figure 4. (a) Schematic of compositional changes from  $\text{Na}_4\text{Si}_{24}$  (left) to  $\text{Si}_{24}$  (right). Na atoms are shown in purple and silicon in yellow. (b)  $\text{Si}_{24}$  unit cell exhibiting three crystallographically unique positions in each color (c) Fractional view of  $\text{Si}_{24}$  emphasizing its channel structure. Channels are formed by eight-member rings along the a-axis, which are linked by six-membered rings on the top and sides. These channels are connected along the c-axis by five-membered rings.

By exposing the recovered  $\text{Na}_4\text{Si}_{24}$  samples to elevated temperatures, removal of Na atoms from the structure was observed. This process occurs at temperatures as low as 320 K, while type-II silicon clathrates ( $\text{Na}_x\text{Si}_{136}$ ) require much higher temperatures ( $> 623$  K) for Na removal. Thermal “degassing” of  $\text{Na}_4\text{Si}_{24}$  at 400 K under dynamic vacuum conditions resulted in a gradual reduction of the sodium content and sodium was completely removed from structure over a period of eight days. The structure of the resulting Na-free structure is unchanged (Cmcm), however, the lattice constants are slightly modified. We verified the absence of Na from the structure using powder X-ray diffraction and energy dispersive X-ray spectroscopy. No sodium was found within our instrumental detection limits (0.1 atom%), therefore, the new structure may be considered as a new allotrope of silicon.

We investigated the electronic and optical properties of the  $\text{Si}_{24}$  allotrope using a combination of experimental and theoretical methods (Figure 5). The new structure possess a quasidirect bandgap of  $\sim 1.3$  eV, which suggests that this structure will be a very useful optoelectronic material. The quasidirect band structure of  $\text{Si}_{24}$  overcomes one of the most fundamental limitations of the “normal” diamond-structured silicon phase, which possesses an indirect band gap.

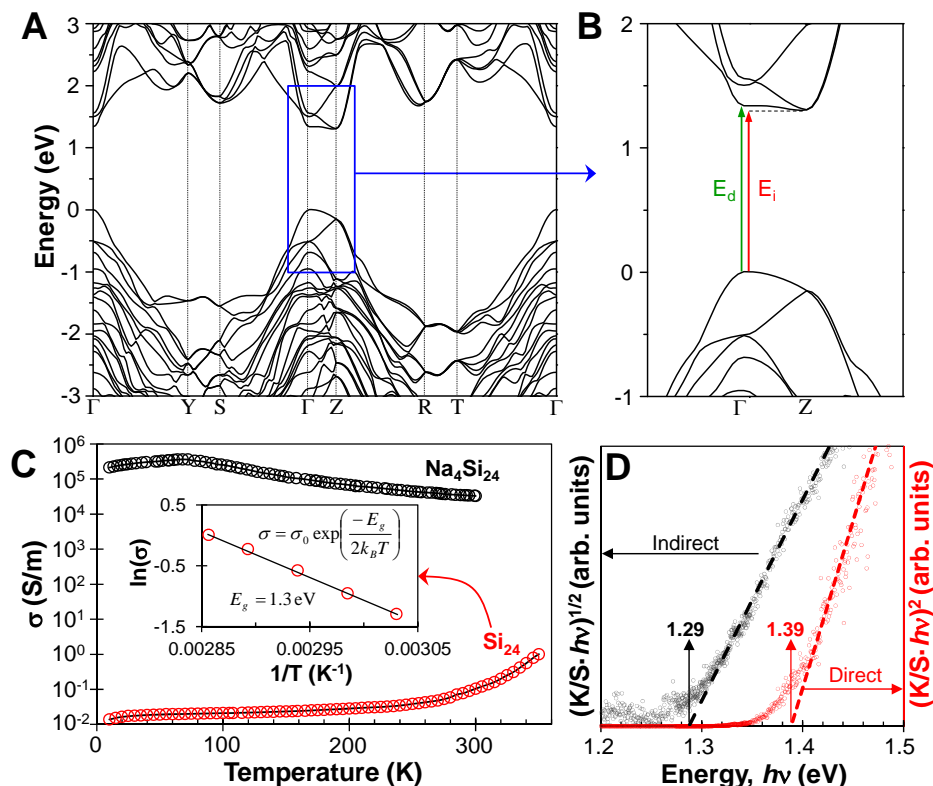


Figure 5. Electronic and optical properties of  $\text{Si}_{24}$ . (a) Calculated  $\text{Si}_{24}$  band structure (PBE). (b) Zoomed in region of band gap with table showing DFT (PBE) and G0W0 corrected values. Arrows indicate direct ( $E_d$ ) and indirect ( $E_i$ ) gaps. (c) Electrical conductivity of  $\text{Na}_4\text{Si}_{24}$  and  $\text{Si}_{24}$  (inset shows fit of intrinsic conductivity region with band gap of 1.3 eV). (d) Tauc plots of Kubelka-Munk absorption ( $K/S$ ) for  $\text{Si}_{24}$  obtained from optical reflectivity measurements. Absorption edges are observed at 1.29 eV and 1.39 eV assuming indirect and direct transitions, respectively

#### 4) Carbon + light metal systems show rich behavior under HP/HT conditions. Several previously unreported structures and compounds were discovered.

The phase behavior and structural evolution of several carbon + light metal systems were investigated under HP/HT conditions. Sources of carbon have included glassy amorphous carbon, nano carbon and graphite, while lights metals have been limited to Li, Mg, Na, and Ca. Results are summarized as follows:

- Below 5 GPa the formation of  $\text{Li}_2\text{C}_2$  (known carbide phase) was observed. Above 12 GPa, at least one new phase was discovered in the Li+C system. Figure 6 shows x-ray diffraction and Raman spectra obtained from this phase, which cannot be described by any know Li+C compounds. Raman modes observed near  $1200\text{ cm}^{-1}$  may be indicative of  $\text{sp}^3$ -type carbon bonding. All of the phases determined thus far are recoverable to ambient conditions.

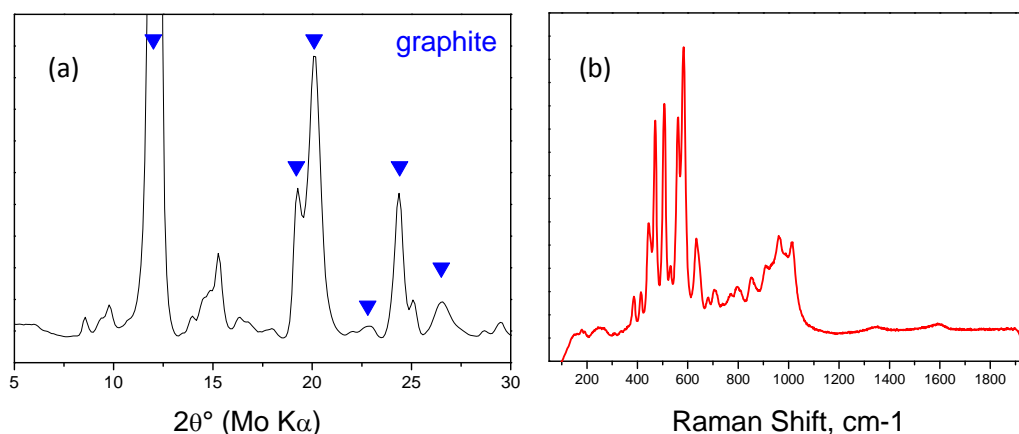


Figure 6. (a) X-ray diffraction pattern showing new peaks for Li+C structure. (b) Raman spectrum Li+C phase synthesized at 12 GPa.

- Up to 20 GPa, we have only observed the formation of the known carbide  $\text{Na}_2\text{C}_2$  in the Na+C system.
- Below 5 GPa the formation of  $\text{CaC}_2$  (known carbide phase) was observed. Above 7 GPa several new phases were discovered (see below).
- The Mg+C system was studied extensively – two new recoverable HP phases were discovered (see below).

**5) A new carbide,  $\text{Mg}_2\text{C}$ , was discovered at HP/HT conditions. This phase is fully recoverable to ambient conditions. It has a bulk modulus of 87 GPa and is electrically insulating. This compound could potentially act as a solid-based fuel source as it is readily hydrolyzed to form  $\text{CH}_4$  gas.**

The Mg+C carbon was investigated over a broad range of synthesis conditions: 7-70 mol% Mg, 1-30 GPa and 500-2000 K. Various sources of carbon have been tested, including glassy amorphous carbon, nano carbon and graphite. At the composition 66 mol% Mg and pressure above 15 GPa, the formation of nearly phase-pure  $\text{Mg}_2\text{C}$  was discovered. Figure 6 shows an xrd pattern obtained from a synthesis run recovered from 15 GPa and ~1700 K and the corresponding  $\text{Mg}_2\text{C}$  structure. Confirmation of the  $[\text{C}^{4-}]$  methanide ion was performed by hydrolyzing samples, which produced  $\text{CH}_4$  gas.

Figure 7 shows the crystal structure of  $\text{Mg}_2\text{C}$  and structural coordination. Carbon within  $\text{Mg}_2\text{C}$  is 8-fold coordinated by magnesium, whereas carbon coordination within  $\text{Mg}_2\text{C}_3$  and  $\text{MgC}_2$  is much more sophisticated. If one considers the whole carbon anions as structural units,  $\text{Mg}_2\text{C}_3$  and  $\text{Mg}_2\text{C}$  have the same coordination number 8, but in the first case they form a distorted and elongated dodecahedron, while in the second case the coordination polyhedron is a regular

cube. In  $\text{MgC}_2$  the  $\text{C}_2$  dumbbell coordination number is 6 (elongated octahedron). Contrary to  $\text{Mg}_2\text{C}_3$  and  $\text{MgC}_2$ ,  $\text{Mg}_2\text{C}$  does not contain covalent C-C bonds. Rather, carbon exists in a very unusual  $\text{C}^{4-}$  ionic state.

The  $^{13}\text{C}$  NMR spectrum (Fig. 7c) of  $\text{Mg}_2^{13}\text{C}$  sample (99% of isotopic purity) displays one resonance at  $\delta+102$  ppm. This agrees with the antifluorite structure which contains only one unique crystallographic position for carbon. The chemical shift is significantly higher than that of  $\text{C}^{4-}$  in  $\text{Al}_4\text{C}_3$  (34 and 51 ppm for C atoms in two crystallographically different sites), and agrees well with higher degree of covalent character of Al-C bonding as compared with Mg-C. The absence of J-coupling in the observed NMR spectrum suggests that carbon within the compound is primarily ionic; increased covalency would be manifested by the presence of J-coupling.

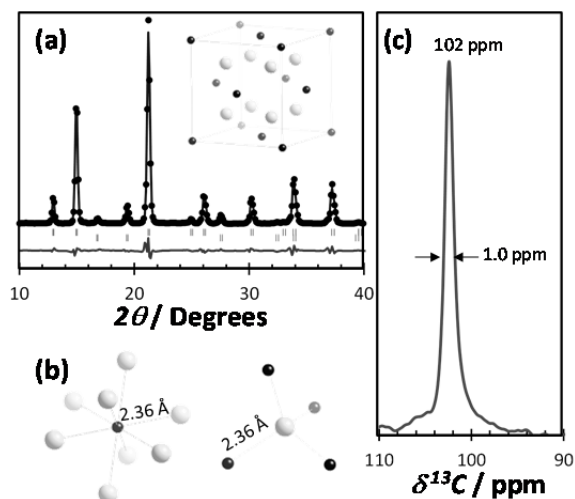


Figure 7. (a) X-ray diffraction data with Mo K radiation (points), Rietveld refinement (line), difference (lower line). Tick marks are shown for  $\text{Mg}_2\text{C}$  (top) and  $\text{MgO}$  impurity (bottom). (b) Carbon and magnesium coordination in  $\text{Mg}_2\text{C}$ . (c) NMR spectrum of  $\text{Mg}_2^{13}\text{C}$  (99% of isotope purity).

To gain further insights into the ionic chemical bonding, we calculated the electron density in the structure and performed a Bader-type bonding analysis (Fig. 8). These results confirm the highly ionic nature of the solid: the effective charges on Mg and C are +1.57 and -3.14, respectively. To our knowledge, this is the most negative effective charge of carbon ever achieved, while the  $\text{C}^{4-}$  ionic radius in  $\text{Mg}_2\text{C}$  has the highest value of 1.50 Å. The magnesium charge is the lowest among other known carbides (+1.65 and +1.7 for  $\text{Mg}_2\text{C}_3$  and  $\text{MgC}_2$ , respectively). The charge density in the (110) plane shows a nearly spherical distribution of electrons centered at Mg and C ions with a low electron density in the interstitial regions (Fig. 8a). The electron localization function (ELF, Fig. 8b) provides a closer look at the bonding nature. ELF minima observed between Mg and C atoms confirm the closed-shell ionic nature of the bonding. There is no "shared-electron" picture, which is characteristic of covalent bonding and requires ELF maxima between atoms.



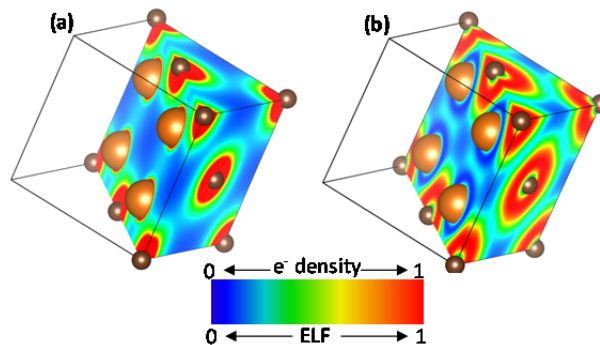


Figure 8. (a) Normalized electron density distribution in  $\text{Mg}_2\text{C}$ , colored blue to red (scale 0 to 1). (b) Electron localization function. Delocalized to localized electrons (ELF) colored from blue to red (scale from 0 to 1). Small and large spheres represent carbon and magnesium, respectively.

The  $\text{C}^{4-}$  character of this compound is very interesting. Although ionic, this carbon exists in an  $\text{sp}^3$  hybridized state and is stable at ambient conditions. We speculate that  $\text{Mg}_2\text{C}$  will serve as a very valuable precursor for the formation of diamond-like  $\text{sp}^3$  carbon at reduced pressure conditions. A direct analogy may be drawn between  $\text{Mg}_2\text{C}$  and Zintl precursors like  $\text{Na}_4\text{Si}_4$ , which are known to form  $\text{sp}^3$  clathrate structures at ambient pressure upon thermal decomposition (despite the fact that the clathrates are only thermodynamically stable at high pressure).

#### 6) The thermodynamic properties of $\text{Mg}_2\text{C}$ were established and the conditions of high-pressure, high-temperature stability have been determined.

The high-pressure and high-temperature stability of antiferite  $\text{Mg}_2\text{C}$  was studied by using in situ X-ray diffraction up to 20 GPa and 1550 K. A combination of *ab initio* calculations of relative energies and phonon density of states as a function of pressure insights to the formation of  $\text{Mg}_2\text{C}$  under extreme conditions and ability to recoverability it at ambient conditions. Our results indicate that high pressure is a crucial point for the thermodynamic stabilization of  $\text{C}^{4-}$  anion in the antiferite structure, although this anion is fully recoverable to ambient conditions.

Figure 9 shows a sequence of in situ X-ray powder diffraction patterns of Mg-C sample, taken during compression to 18 GPa (at 300 K), with heating to 1550 K (at ~18 GPa) and subsequent isothermal decompression (at ~1550 K). The formation of  $\text{Mg}_2\text{C}$  was observed during heating at 18 GPa after the non-equilibrium melting of Mg at ~1500 K. At 1550 K  $\text{Mg}_2\text{C}$  decomposes at the pressure of ~12 GPa. A constant composition section (33 at.% C) of the p-T phase diagram of  $\text{Mg}_2\text{C}$  was established using our in situ data at 1550 K and the 0 K value predicted by *ab initio* calculations (stability compared to Mg-diamond mixture). The melting temperatures of  $\text{Mg}_2\text{C}$  at 1 MPa and 15 GPa were then estimated using a Lindemann mode combined with *ab initio* calculations of the Debye temperature under pressure and experimental p-V equation of state.

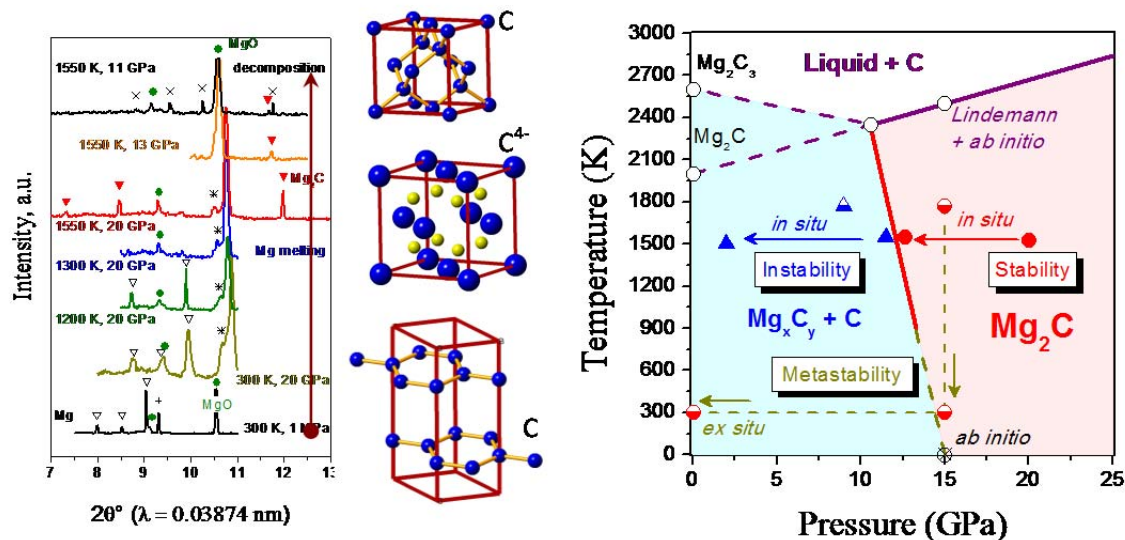


Figure 9. Experimental X-ray diffraction data obtained *in situ* during the HPHT formation of  $\text{Mg}_2\text{C}$  (left). Structures of graphite,  $\text{Mg}_2\text{C}$ , and diamond (center), Phase diagram determined for  $\text{Mg}_2\text{C}$  (right).

**7) A new polymorph of  $\text{Mg}_2\text{C}_3$  carbide was discovered and the crystal structure was solved using a combination of experimental and theoretical methods.**

High-pressure, high-temperature studies were conducted in the Mg+C system at compositions other than  $\text{Mg}_2\text{C}$ , namely,  $\text{Mg}_2\text{C}_3$ . In this case, another structure was identified with a much more complex structure than cubic  $\text{Mg}_2\text{C}$ . With the assistance of *ab initio* structure searching methods, we were able to successfully solve the structure (Figure 10) from *in situ* X-ray data. Like the previously known orthorhombic Pnnm structure ( $\alpha$ - $\text{Mg}_2\text{C}_3$ ), the new monoclinic C2/m structure ( $\beta$ - $\text{Mg}_2\text{C}_3$ ) contains linear  $\text{C}_3^{4-}$  chains that are isoelectronic with  $\text{CO}_2$ . Unlike  $\alpha$ - $\text{Mg}_2\text{C}_3$ , which contains alternating layers of  $\text{C}_3^{4-}$  chains oriented in opposite directions, all  $\text{C}_3^{4-}$  chains within  $\beta$ - $\text{Mg}_2\text{C}_3$  are nearly aligned along the crystallographic c-axis. Hydrolysis of  $\beta$ - $\text{Mg}_2\text{C}_3$  yields  $\text{C}_3\text{H}_4$ , as detected by mass spectrometry, while Raman and NMR measurements show clear C=C stretching near  $1200\text{ cm}^{-1}$  and  $^{13}\text{C}$  resonances confirming the presence of the rare allylenide anion.

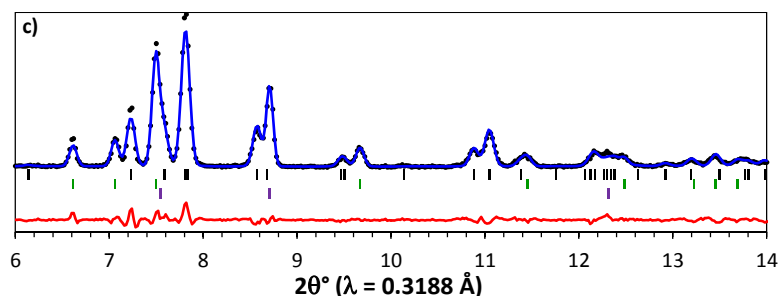


Figure 10. *In situ* angular dispersive diffraction pattern for  $\beta$ - $\text{Mg}_2\text{C}_3$  synthesized in the PE press and recovered to ambient pressure. Rietveld refinement was employed for the  $\beta$ - $\text{Mg}_2\text{C}_3$  structure, while Le Bail analysis was used for MgO and Mg due to strong preferred orientation



caused by recrystallization and capsule texture. Tick marks indicate  $\beta$ - $\text{Mg}_2\text{C}_3$ , Mg and MgO from top to bottom.

The new  $\text{Mg}_2\text{C}_3$  structure is monoclinic with space group  $C2/m$  with  $a = 4.8$ ,  $b = 4.7$ ,  $c = 6.0$  Å and  $\beta = 126^\circ$ . This phase forms above  $\sim 6$  GPa and is stable to  $\sim 15$  GPa. Observations suggest that this structure transforms to  $\text{Mg}_2\text{C}$  at higher pressure (with heating and depending on global composition). Unlike  $\text{Mg}_2\text{C}$ ,  $\text{Mg}_2\text{C}_3$  contains linear  $\text{C}_3^{4-}$  chains that are charge balanced by  $\text{Mg}^{2+}$  cations (Fig. 11).

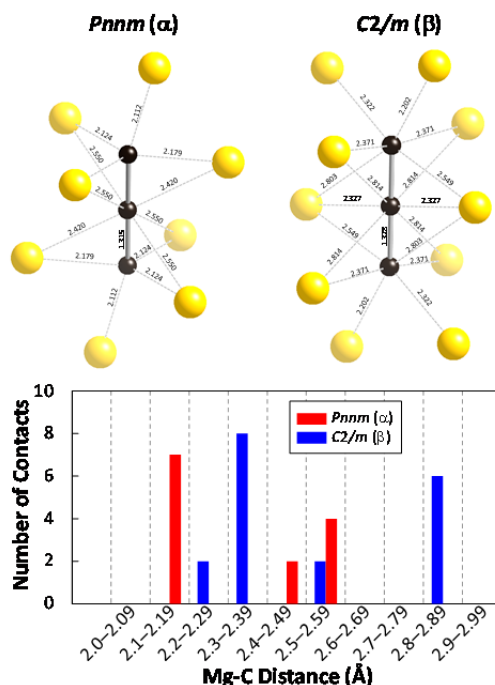


Figure 11.  $\text{C}_3^{4-}$  coordination in  $\alpha$  and  $\beta$   $\text{Mg}_2\text{C}_3$  and histogram of nearest neighbor Mg-C distances out to 3 Å.

## 8) New structures in the Ca+C system were identified. Some of these may contain unique polymeric carbon units.

Studies were performed in the Ca+C system to investigate the influence of Ca on  $\text{sp}^3$  carbon network formation. At pressures  $< 4$  GPa, we observed the formation of  $\text{CaC}_2$  calcium carbide, a known structure with linear  $\text{C}_2^{2-}$  dumbbells. At higher pressure, new structures were identified. Figure 12 shows in situ X-ray diffraction patterns obtained at 20 GPa and 600-900 K. The starting FCC (or BCC depending on pressure) metal clearly transforms into a lower symmetry structure(s).

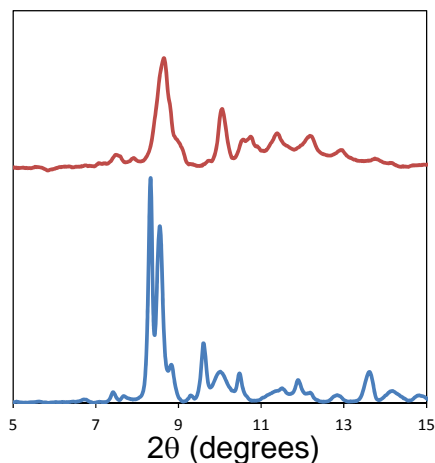


Figure 12. X-ray diffraction patterns obtained for Ca+C mixtures at 20 GPa heated to 600 K (bottom) and 900 K (top). Low symmetry structures are clearly identified.

With the aid of ab initio structural searching, we have identified candidate structures for the new Ca+C compounds. Figure 13 shows possible structure and corresponding XRD patterns that match closest to the experimental data. Both of these structures (P-1 and Immm symmetries) contain 1D carbon nano chains.

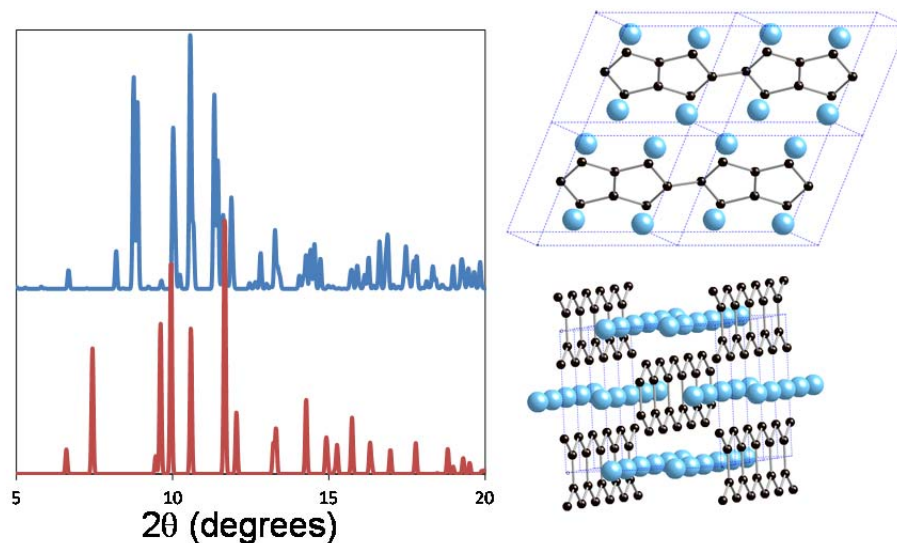


Figure 13. Simulated X-ray diffraction patterns and crystal structures for new  $\text{CaC}_2$  compounds with P-1 symmetry (top) and Immm symmetry (bottom).

These structures are very unique in the sense that they contain polymerized carbon nano-ribbons. These phases should be metallic with very interesting properties. Furthermore, they offer the possibility of extracting 1D carbon nanochains, which may have very interesting mechanical properties.

In addition to this, we have identified three new carbide structures up to 30 GPa, using a combination of X-ray diffraction methods and *ab initio* crystal structure searching (Fig. 14).  $\text{Ca}_2\text{C}$  contains  $\text{C}^{4-}$  anions, similar to  $\text{Mg}_2\text{C}$ , however, the structure is orthorhombic. Monoclinic  $\text{Ca}_2\text{C}_3$  is isostructural with  $\beta\text{-Mg}_2\text{C}_3$ , but no a modification is known for the case of Ca. Finally, an entirely new composition,  $\text{Ca}_3\text{C}_2$ , was discovered. This structure is metallic and does not have formal charge balance.

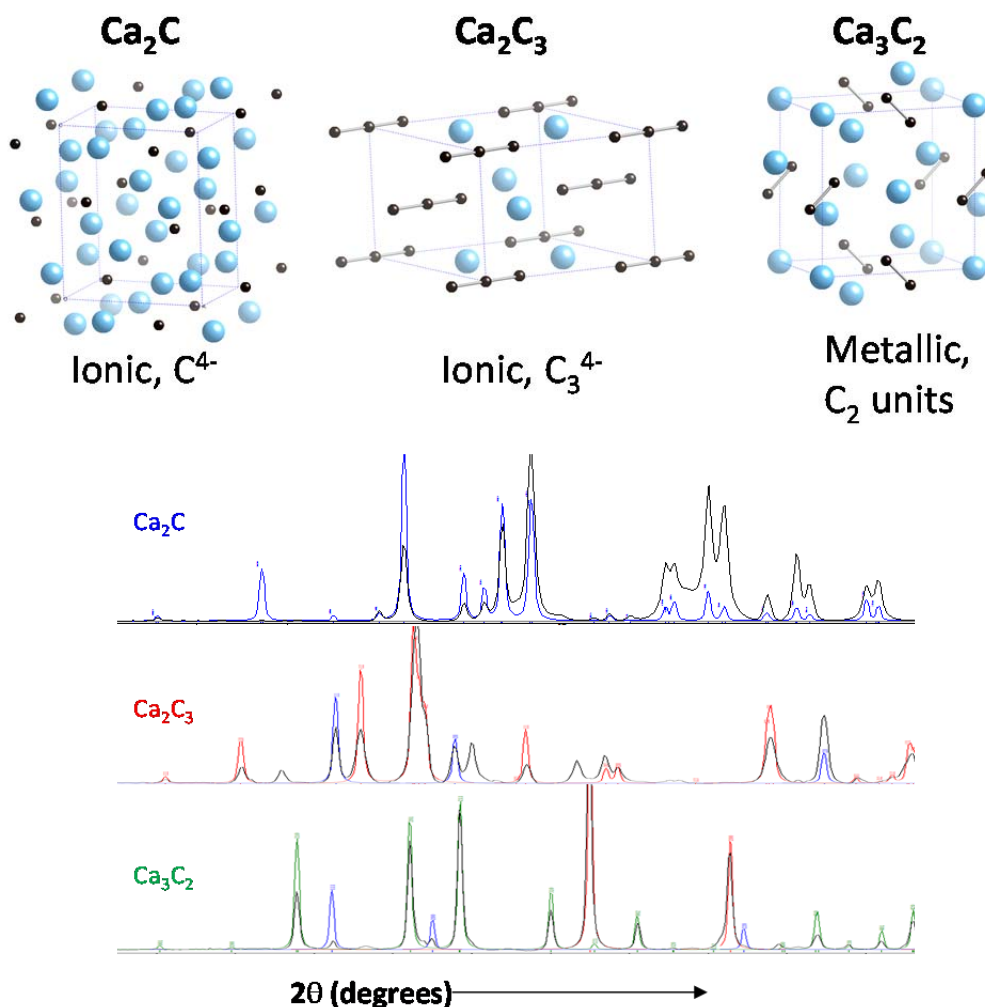


Figure 14. Structures and X-ray diffraction patterns for new Ca-C carbides.

- 9) **Methods were developed to prepare samples of p-CO. This can be done routinely for samples with dimensions of 1000 micron diameter x 150 micron thickness.**

We have developed experimental procedures to load CO into diamond anvil cells (DAC) using both cryogenic and high-pressure gas methods. These techniques are extremely reliable (near 100% loading efficiency). When utilizing the supported anvil design (Boehler-Almax style), large samples may be produced (1000 micron diameter x 150 micron thickness at 7 GPa).

**10) The polymerization pressure of CO in the presence of N<sub>2</sub> and C<sub>2</sub>H<sub>4</sub> is not reduced from the pure CO sample conditions. These dopants tend to phase separate with no significant alteration of the chemical structure; however, subtle vdW-type interaction was observed.**

Experiments were conducted on mixtures of CO and N<sub>2</sub> or C<sub>2</sub>H<sub>4</sub> to determine if polymerization in the presence of these compounds would decrease the polymerization onset pressure or increase the chemical stability through bonding with the p-CO network. Neither of the components was found to reduce the polymerization pressure required for pure CO (~6 GPa at room temperature). Both N<sub>2</sub> and C<sub>2</sub>H<sub>4</sub> exhibited phase separation from p-CO and infrared (IR) spectra obtained from the different samples did not indicate any significant bonding changes in the polymer structure. However, subtle shifts in Raman modes suggest the presence of weak van der Waals interaction. Figure 15 shows images of p-CO with N<sub>2</sub> and C<sub>2</sub>H<sub>4</sub>, as well as the corresponding IR spectra.

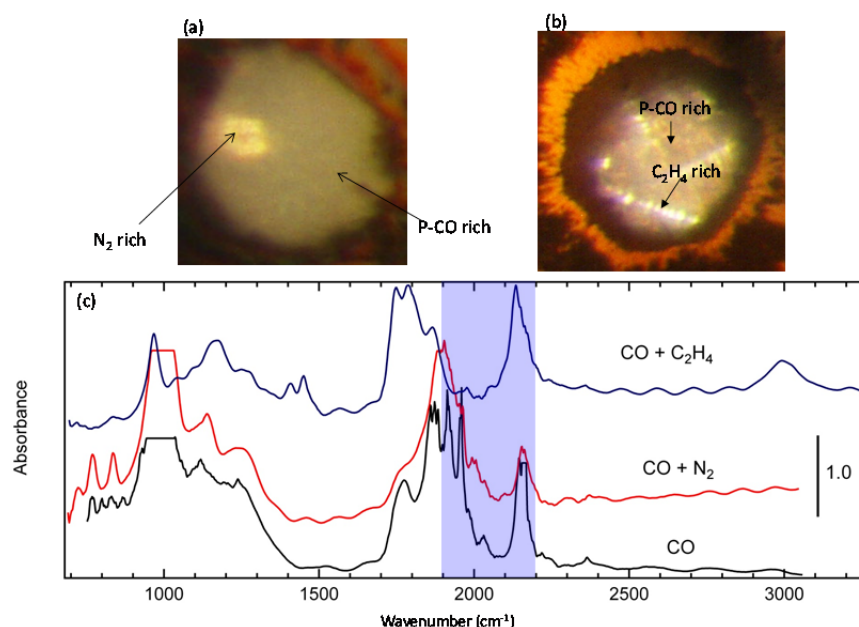


Figure 15. (a) Image of N<sub>2</sub>+p-CO mixture and (b) C<sub>2</sub>H<sub>4</sub>+p-CO mixture showing phase separation of the components. (c) IR spectra for the different samples indicating no significant changes in chemical bonding. For the case of C<sub>2</sub>H<sub>4</sub>, new IR modes appear which originate from pure C<sub>2</sub>H<sub>4</sub>.

**11) Neither seed crystals of p-CO nor nano-sized Pd powder reduce the pressure required for CO polymerization at ambient temperature.**

In order to reduce the polymerization onset pressure for pure CO, attempts were made to catalytically induce (reduce nucleation barrier) p-CO formation using nano-Pd powder and a seed crystal of pure p-CO. Neither of these additives was found to reduce the polymerization onset pressure. Figure 16 shows the seed crystal of p-CO surrounded by molecular CO and corresponding IR spectra.

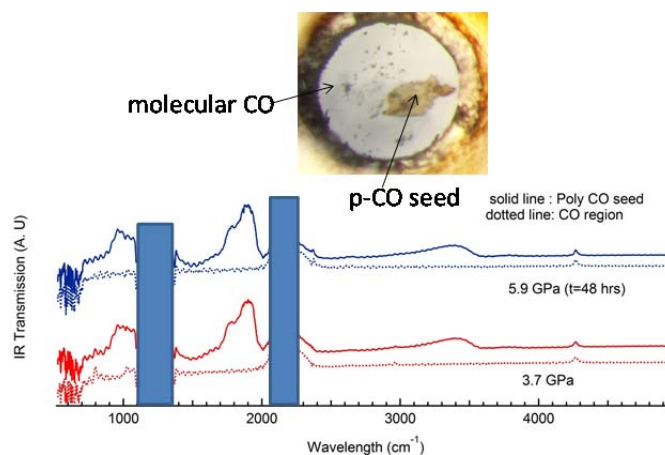


Figure 16. Image of p-CO seed crystal inside diamond anvil cell at 5.9 GPa surrounded by molecular CO. The molecular CO does not polymerize, while in contact with the seed. IR spectra are shown at bottom.

**12) Amorphous carbon appears to reduce the polymerization onset pressure of CO by ~0.5 GPa when compared with the pure system. It is unclear whether this is a catalytic (nucleation) or thermodynamic (chemical stabilization) effect.**

The polymerization of CO was investigated in the presence of amorphous nano-carbon. Compared with pure CO, which always shows a polymerization onset pressure between 5.5-7 GPa depending on the exact experimental conditions, the sample in contact with nano carbon started to polymerize at only 4.8 GPa. This represents an approximate 0.5 GPa decrease in the pressure required for CO polymerization in the pure system. Figure 17 shows an image of the CO in contact with nano carbon and the corresponding IR spectra with pressure. It is unclear whether this process is catalytic in nature or if the carbon plays a chemically stabilizing role. The detailed determination of chemical stability is currently under investigation.

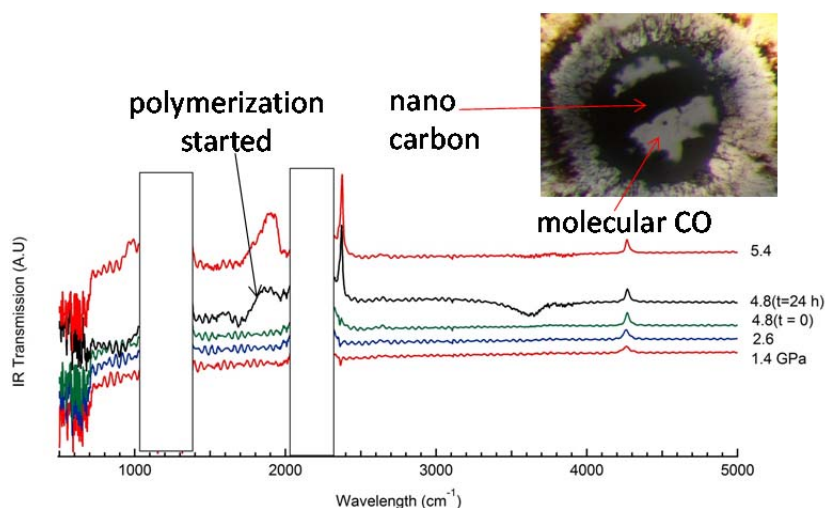


Figure 17. Image of molecular CO in contact with nano carbon before polymerization and IR spectra obtained with increasing pressure indicating polymerization onset at 4.8 GPa.

**13) The polymerization pressure of CO was investigated in the presence of several different metal and non-metal catalysts. Metallic lithium and sodium, as well as non-metallic amorphous carbon and SiO<sub>2</sub>, appear to reduce the pressure needed for CO polymerization.**

We have used a combination of IR and Raman spectroscopy studies to explore the possibility of lowering the polymerization pressure of CO. We undertook three separate routes to systematically explore the lowering of polymerization pressure in CO. In the first study, we attempted to use the fact that several groups that have used diamond anvil cells reported a range of pressures depending on the gasket material. We hypothesized that this could indicate metal-CO interaction and therefore a dependence of this interaction on the polymerization pressure.

We chose to standardize the protocol by using Au lined stainless steel gaskets and IR spectrometry using the pressure shift of the antisymmetric NO<sub>2</sub> stretch as a pressure sensor and the appearance of carbonyl bands (at 720 cm<sup>-1</sup>) and the epoxy bands (at 830 cm<sup>-1</sup>). This was necessary to reduce the effect of photo-reactivity and also establish the formation of the correct polymeric phase. To strengthen the signal from the sample and proper referencing, we used gaskets with dual holes, one filled with the KNO<sub>2</sub>-KBr mixture and the other completely filled with CO. The gasket geometry was first calibrated using ruby and N<sub>2</sub> in the sample chamber instead of CO.

Once this protocol was established, we used several metal additives such as nano-Pd, Pt, Pt-black, Al, Na, Li as well as common gasket materials such as Re, W, Fe and Cu. We also tested non-metallic additives of amorphous carbon and SiO<sub>2</sub> (Fig. 18).

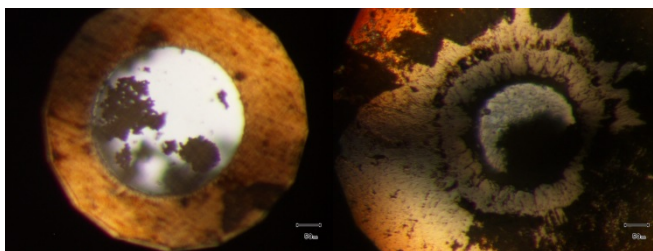


Figure 18. The panel on the left shows CO loaded along with Pd sponge and the panel on the right shows CO with Na dispersed in the sample chamber. Both the samples were photographed at low pressures prior to polymerization. The gasket material used in both cases is Be-Cu.

Interaction between CO and non-metals such as C and SiO<sub>2</sub> but with large surface area of contact such as glassy, nano-carbon, silica wool, carbon nanotubes

While no appreciable decrease in polymerization pressure or changes in the spectroscopic characteristics of the polymeric phase were observed in most cases, a modest reduction in the polymerization pressure was observed for amorphous carbon and SiO<sub>2</sub>. These studies have consistently shown reduction of polymerization pressure by at ~1 GPa and the resultant polymeric phase shows all the signatures reported previously.

Appreciable drop in polymerization pressure was also observed in the case of Li when mediated by slight increase in temperature. While in the case of Li, the polymerization pressure dropped to 1 GPa, in the case of Na, it dropped to 2 GPa when mediated with photo-reactivity of incident 532 nm or 488 nm laser radiation. When the experiment was repeated using 660 nm radiation, no change in polymerization pressure was observed.

X-ray diffraction of the polymerized products revealed a majority polymeric phase admixed with a small amount of crystalline phase that was not pure Na or Li indicative of a chemical reaction (Fig. 19). This could imply that the polymerization is indeed aided by interaction between the alkali metals and CO and further that the activation energy involved could be lowered either by increasing the surface of contact or temperature (photo-induced).

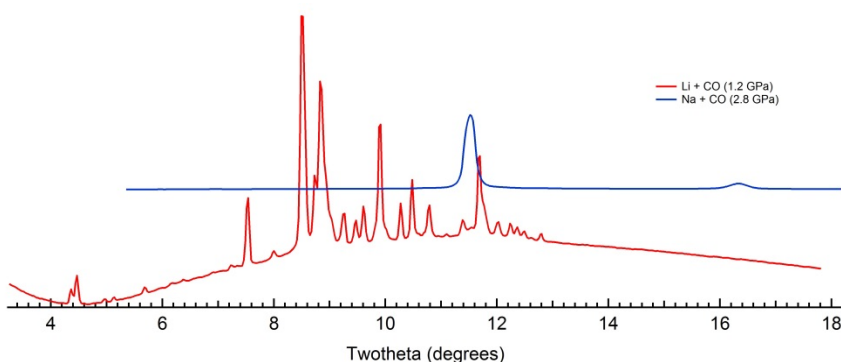


Figure 19. The integrated diffraction patterns of the polymeric phase obtained with Li at 1 GPa and Na at 2.8 GPa. The broad peak weak signal is detected in both from the amorphous polymer. For Li, a crystalline phase was observed, which indicates a complicated large unit cell structure not similar to Li at this pressure (1.2 GPa).